Electronic Supplementary Material (ESI) for Lab on a Chip.
This journal is © The Royal Society of Chemistry 2017

SUPPLEMENTARY INFORMATION FOR:

Characterizing the effects of anticancer peptides at the single cell level within picoliter-sized microfluidic chambers

L. Armbrecht,[a] G. Gabernet,[b] F. Kurth,[a] J. A. Hiss,[b] G. Schneider[b] and P. S. Dittrich[a]

a. Department of Biosystems Science and Engineering, ETH Zurich, Switzerland.

b. Department of Chemistry and Applied Biosciences, ETH Zurich, Switzerland.

Supplementary Figure S1.

Fabrication of the master mold by soft-lithography of SU-8 2015 on 4" Si-wafers.

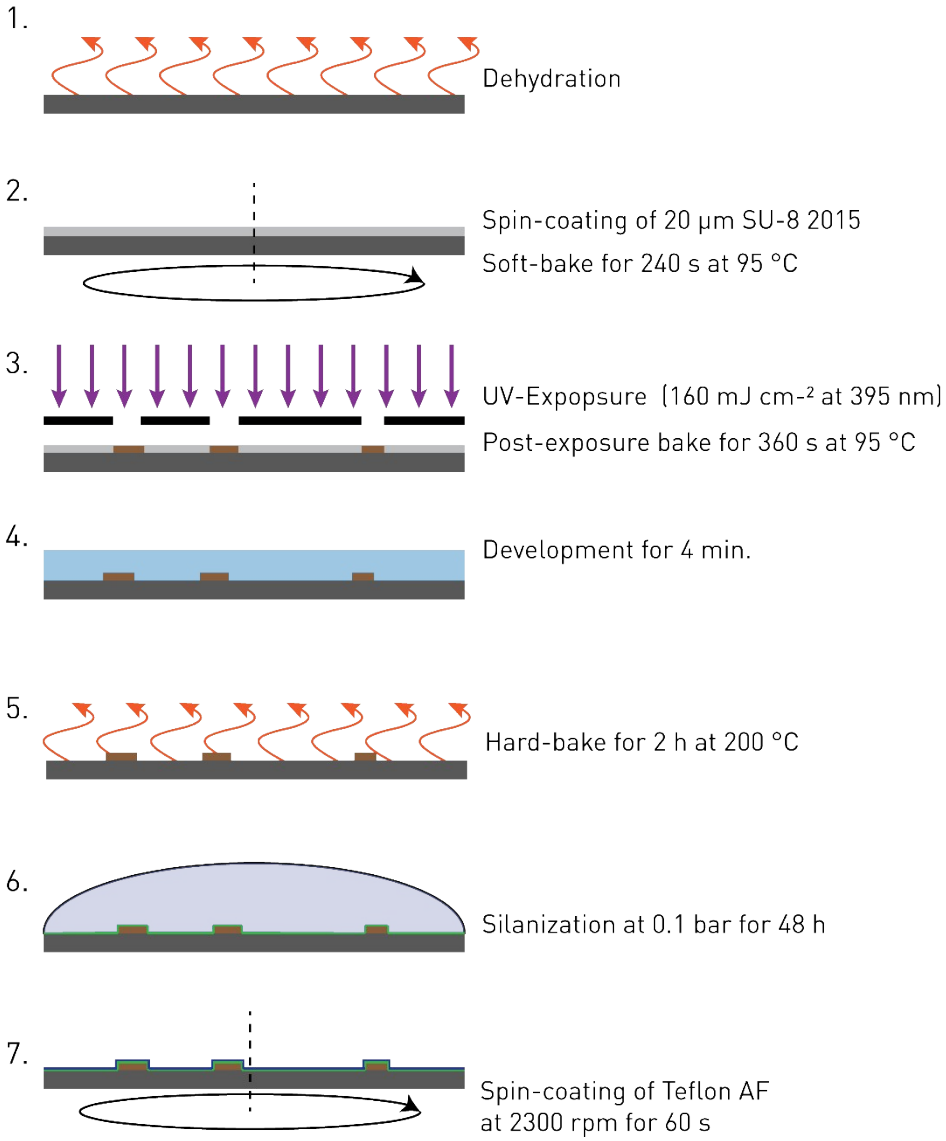

Supplementary Figure S2.

Microfluidic PDMS chip fabrication from the silicon master molds.

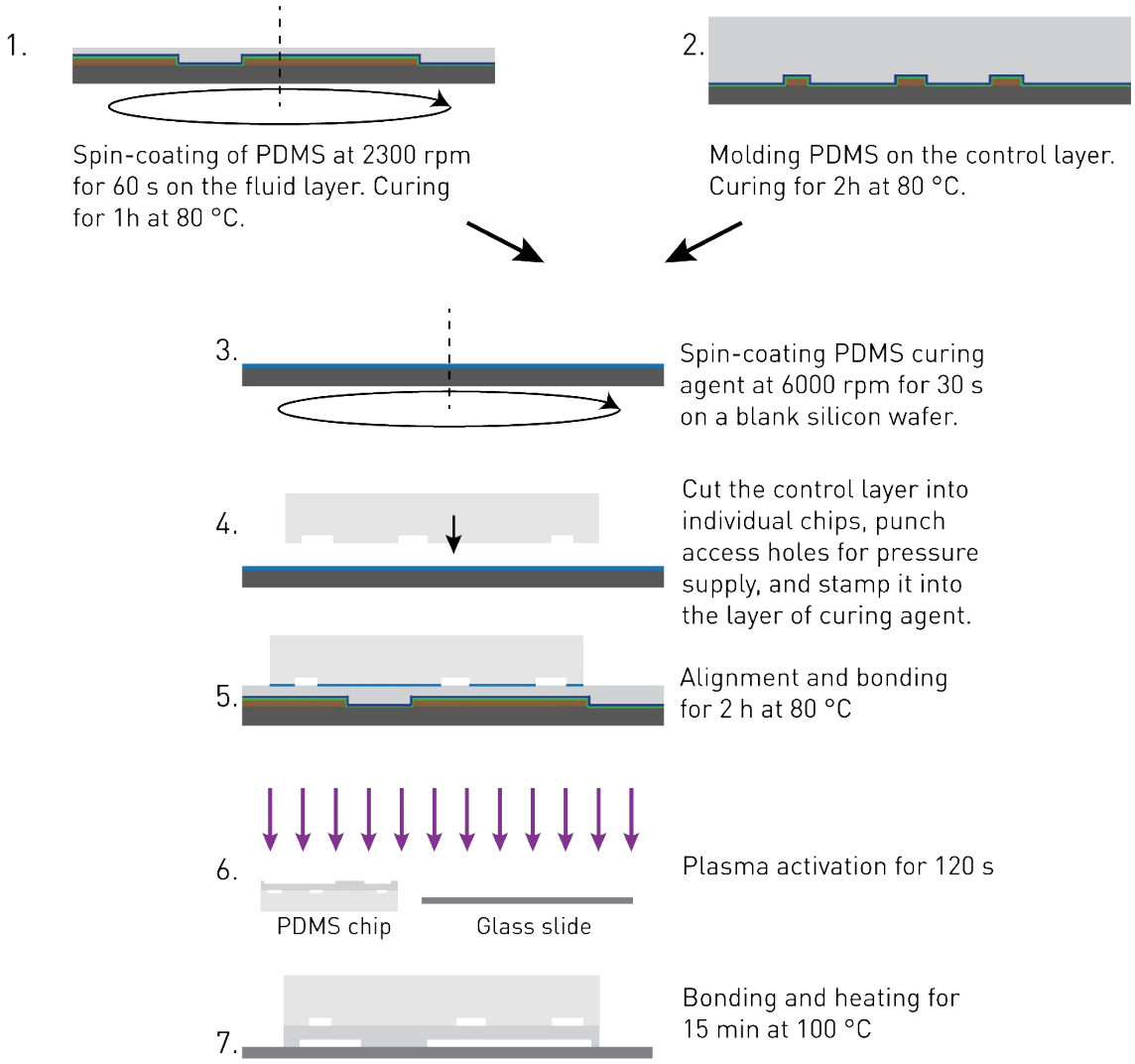

Supplementary Figure S3.

The microfluidic chip can be divided into three sections (A). The first section (orange) is the inlet and a filter with gap sizes of 30 µm. Cell agglomerates are typically flexible such that multi-cell clusters can pass the filter structure. This is followed by a short section (green), where the channel widens up to its maximum width and connects to the third section (red) that holds the single cell traps and doughnut-shaped valves. Pillars placed in sections two and three prevent the channel from collapsing due to the flexible properties of PDMS. The chamber region consists of 34 rows each containing 18 cell traps. A close-up of one cell trap including the valve and adjacent supporting pillars is depicted in B. To improve cell capture efficiency, the traps in each subsequent column are shifted 20 µm sideways compared to the previous column thereby probing the whole channel cross section. The complete design including all dimensions can be found in the appended CAD file (SF1).

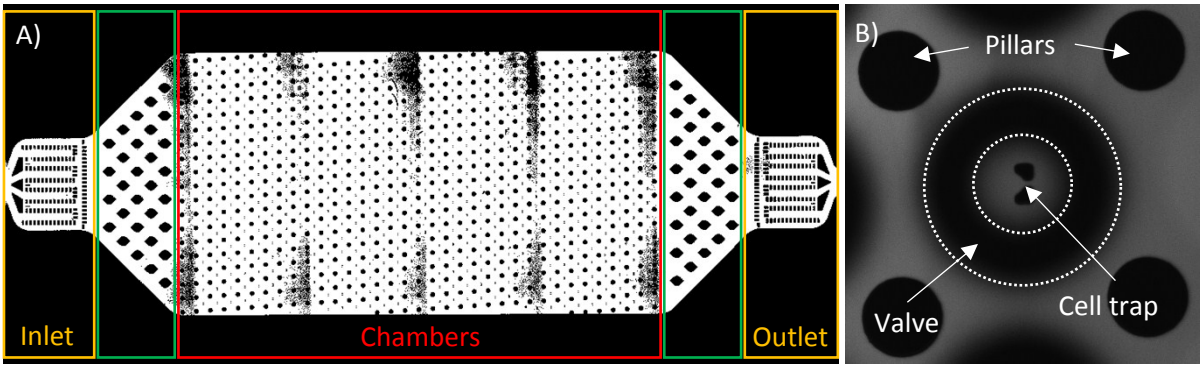

Supplementary Figure S4.

Applying pressures equal to or higher than 1.5 bar is sufficient to completely seal the chambers from the surrounding medium (bottom). To prove this, we added 50 µM Fluorescein solution into the microfluidic channels and actuated the pneumatic doughnut shaped valves. A reference background signal was measured outside of the fluorescent microchannel and compared to the fluorescent signal at the valves. For pressures of at least 1.5 bar, the fluorescent signal at the valves drops to the background level. This indicates complete isolation of the chambers.

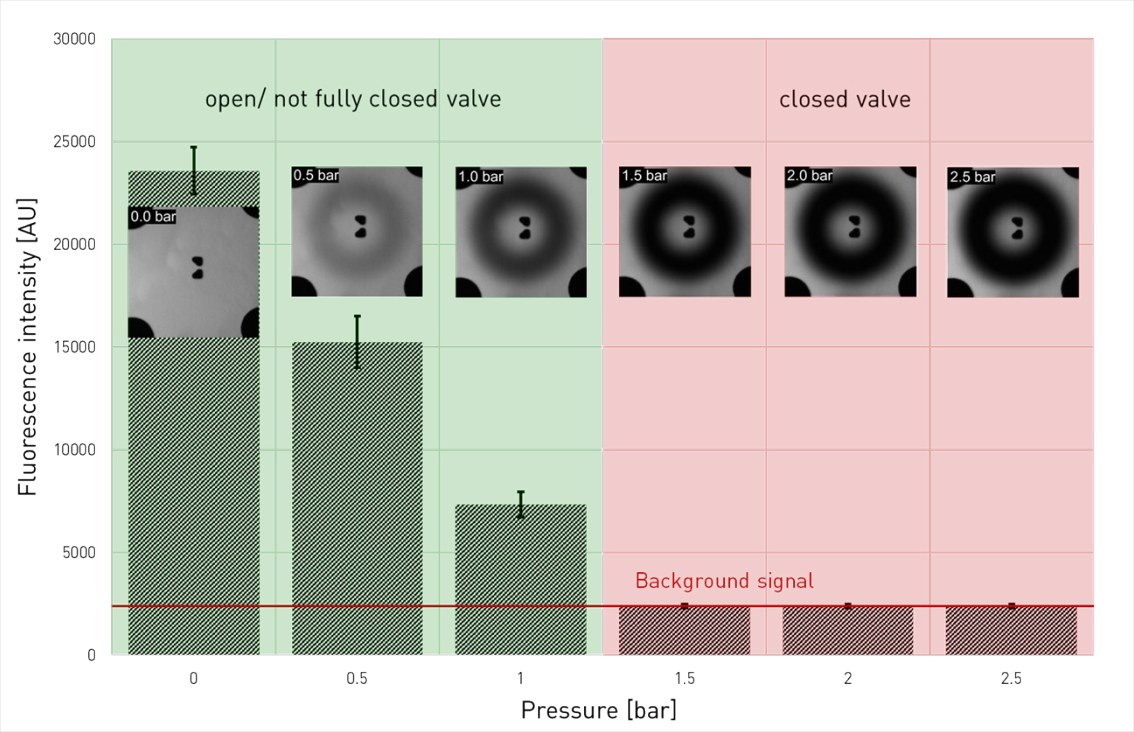

Supplementary Figure S5.

The volume of the closed microfluidic chambers can be calculated assuming cylindrical shape of the valve and a chamber diameter as designed to 100 µm. This results in a theoretical volume per chamber of 157 pL. Filling the chambers with fluorescein solution (50 µM) and taking images of the closed chambers reveals the real shape of the chamber (fluorescence intensity scales linearly with chamber height). Based on these results, the chamber volume can be calculated to 93 pL. The reason for the difference to the theoretical volume is the deformation of the PDMS valve due to the applied pressure.

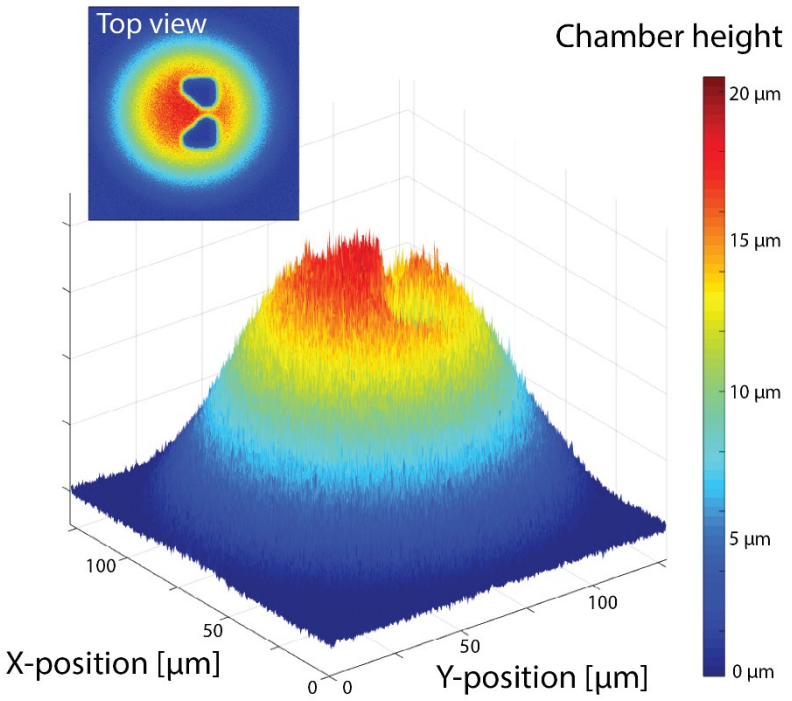

Supplementary Figure S6.

A) Comparison of the cell viability after 6 h on and off-chip. The heating of the custom heating stage was found to reach 37 ˚C after 15 min (B). The standard deviation includes both, deviations from different runs as well as measurements at different locations in throughout the microfluidic chamber. Mounted onto the microscopy setup (C), the device (D) is low-cost, robust and can be easily migrated from one microscope to another.

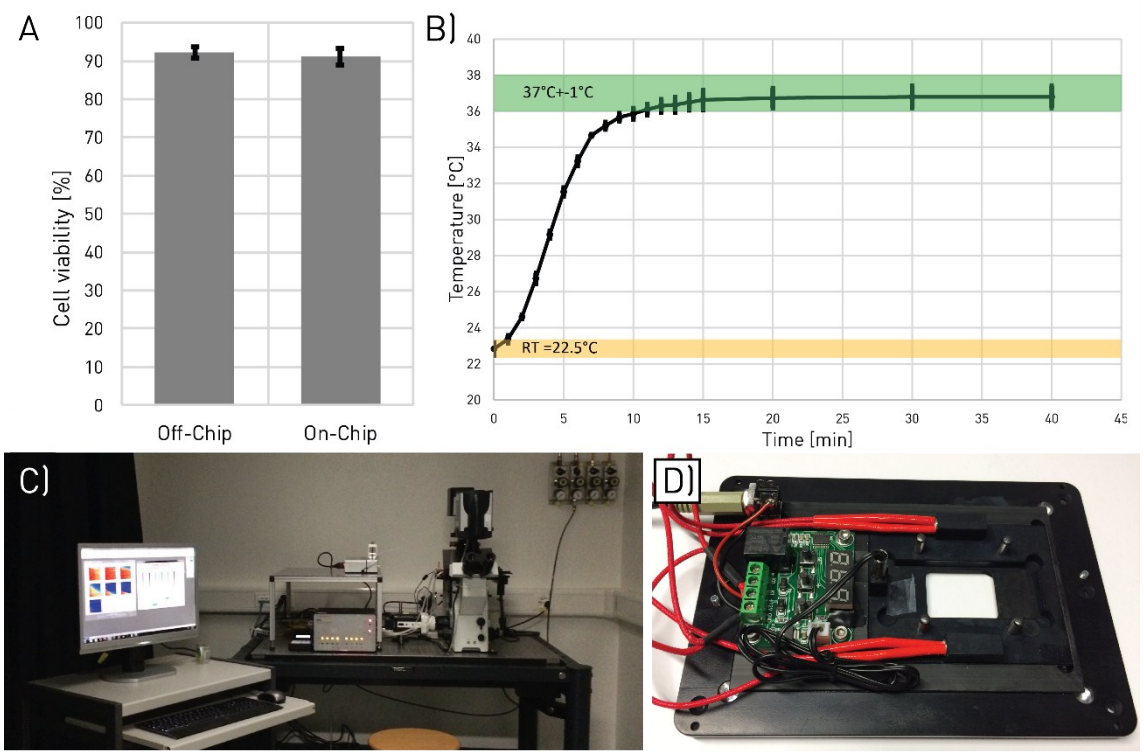

Supplementary Figure S7.

Post processing of long-term imaging data. A stacked image of the complete trapping area (top) is evaluated by tracking each single cell over time (full time series in SV3). The image set below shows a time series of a small section of the cell capturing channel with nine individual cell traps. The cells on the top right and bottom left of this section are multi-cell clusters and excluded from analysis. All single cell signals are evaluated for every time point, whereby the fluorescent intensity decreases upon membrane disruption. The resulting single cell time-lapse data is finally sorted and displayed in a 2D-matrix as shown in Fig. 2, 4 and S9.

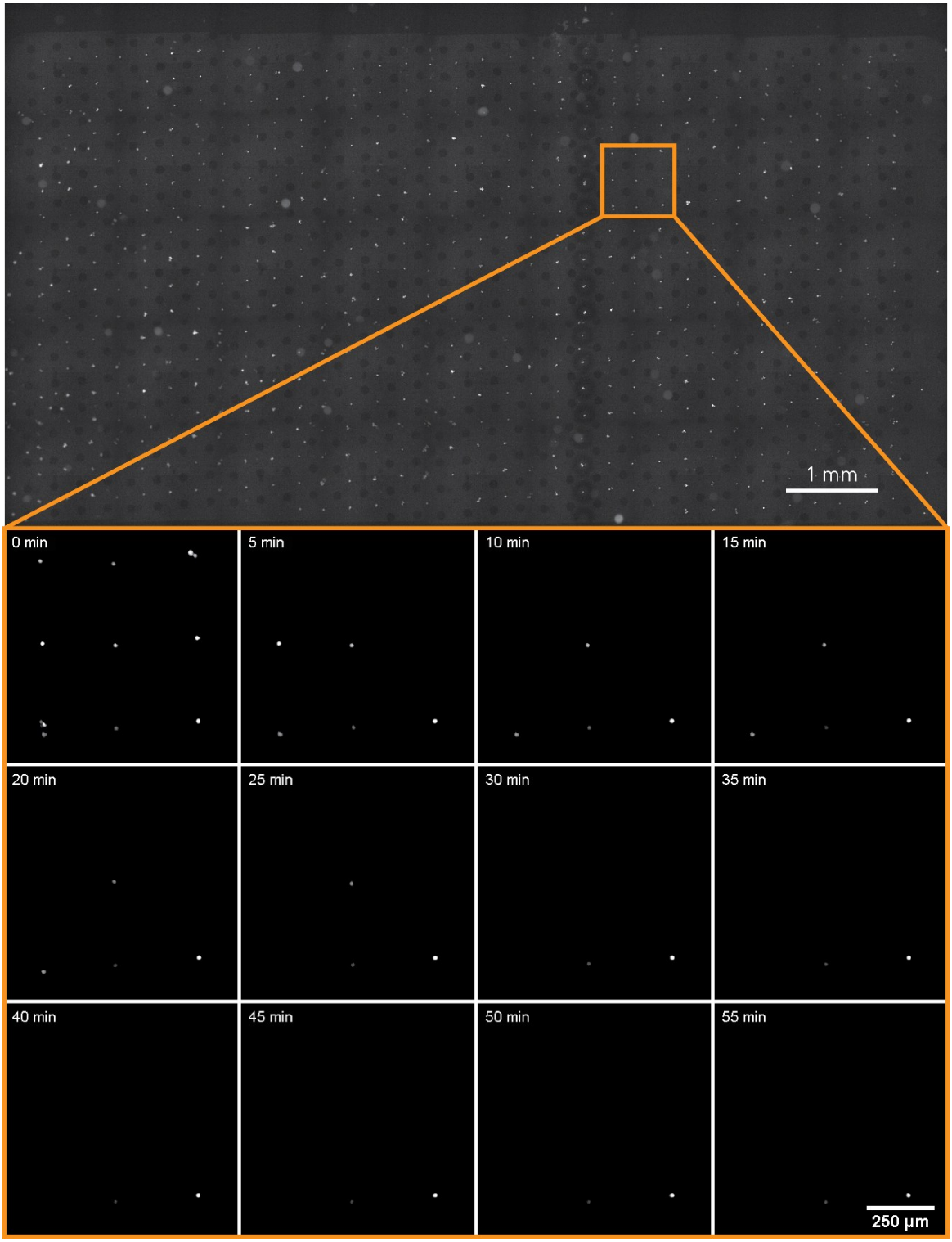

Supplementary Figure S8.

Determination of the half effective concentration (EC50) of Melittin, Aurein 1.2 and Aurein 2.2 in an MTT assay. This value was 1.83 ± 0.08 µM for Melittin (A), 44.77 ± 2.65 µM for Aurein 1.2 (B), and 34.77 ± 3.25 µM for Aurein 2.2 (C). The gray area corresponds to the standard error of the fit of a 3-parameter log-logistic model.

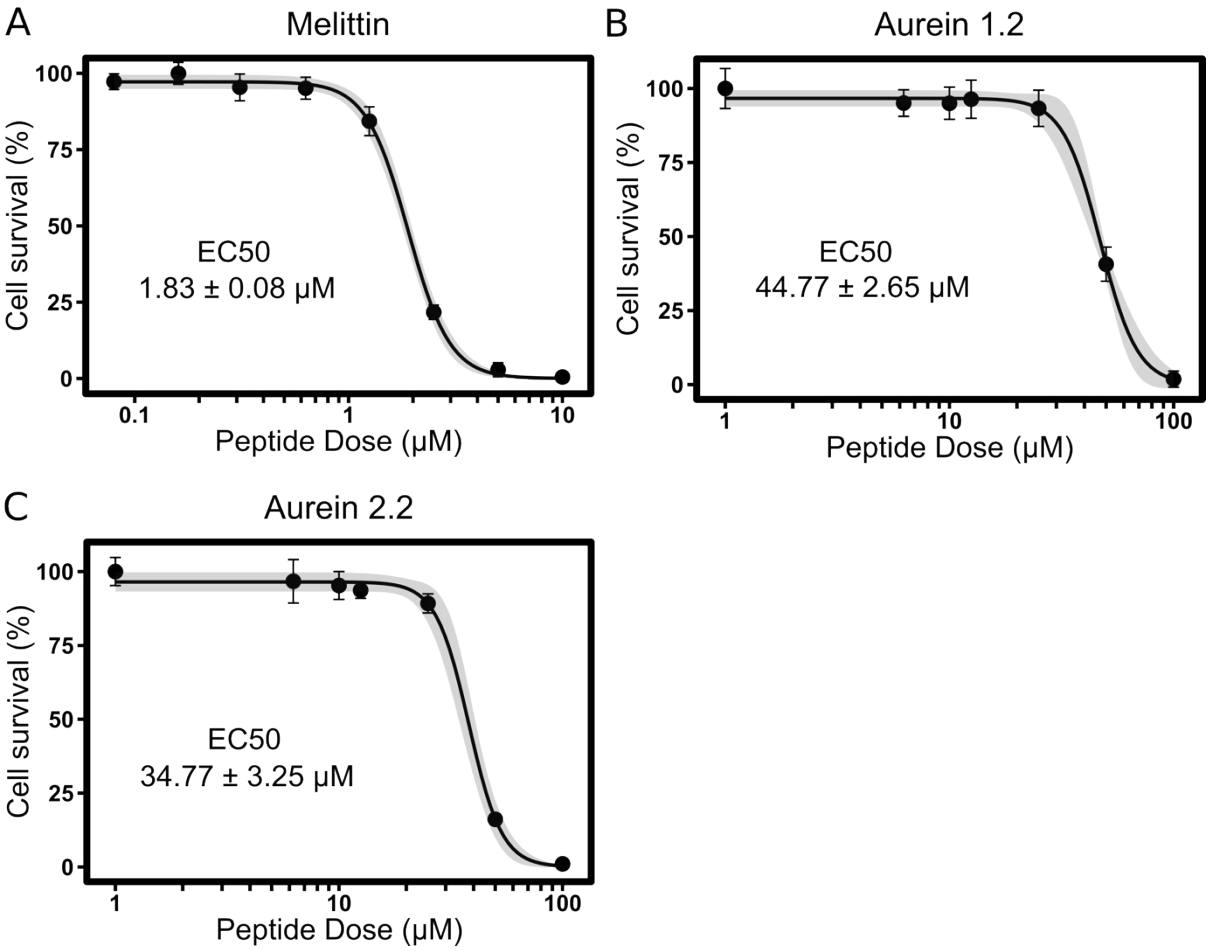

Supplementary Figure S9.

Bleaching of calcein-AM stained cells was seen to be pronounced during continuous light exposure. A reduction to 50 % of the fluorescence occurred after 250 s (top). To monitor individual single cells at high temporal and spatial resolution, we limited the experiments to 100 s to keep bleaching effects at an acceptable level. For long-term high-throughput experiments, the cells were exposed to light only for 100 ms at each measurement time point thereby reducing the total light dose to an equivalent of 6 s continuous illumination (bottom). Here, the bleaching is much slower and we can clearly determine the time point of the membrane lysis characterized by the fast drop in the calcein fluorescence.

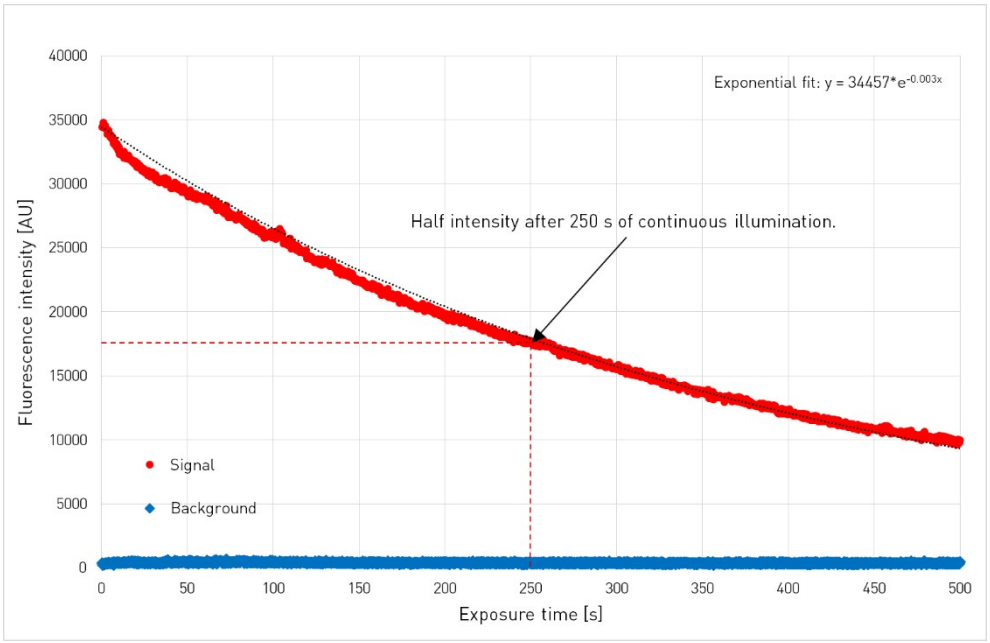

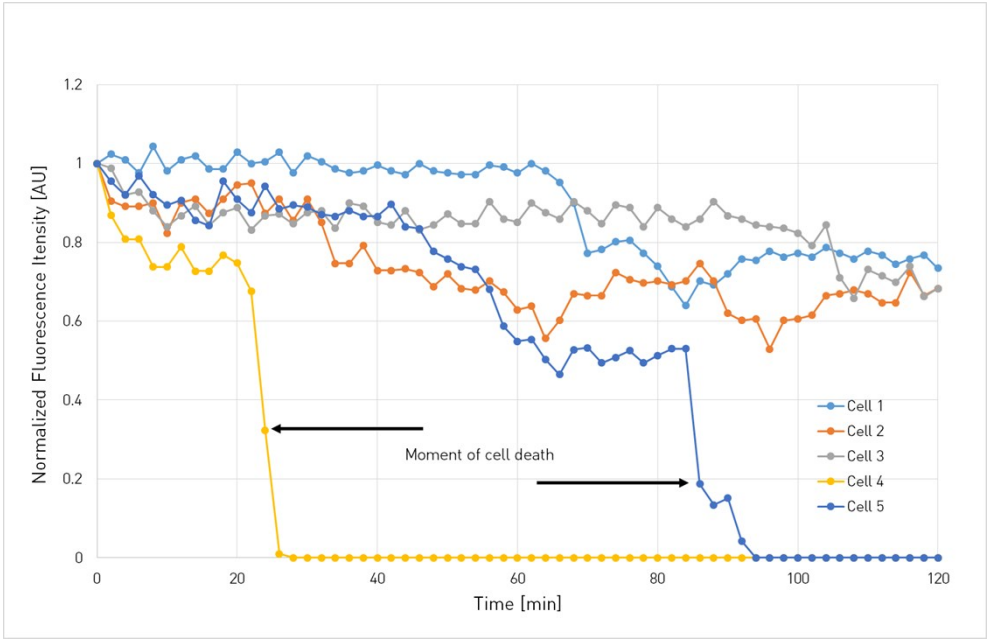

Supplementary Figure S10.

2D-matrix plots for all tested Aurein 2.2 peptide concentrations including the control (0 µM Aurein 2.2). Total number of analyzed cells: n(control) = 173, n(10 µM) = 162 , n(20 µM) = 221 , n(30 µM) = 174, n(40 µM) = 174, n(50 µM) = 269, n(60 µM) = 191.

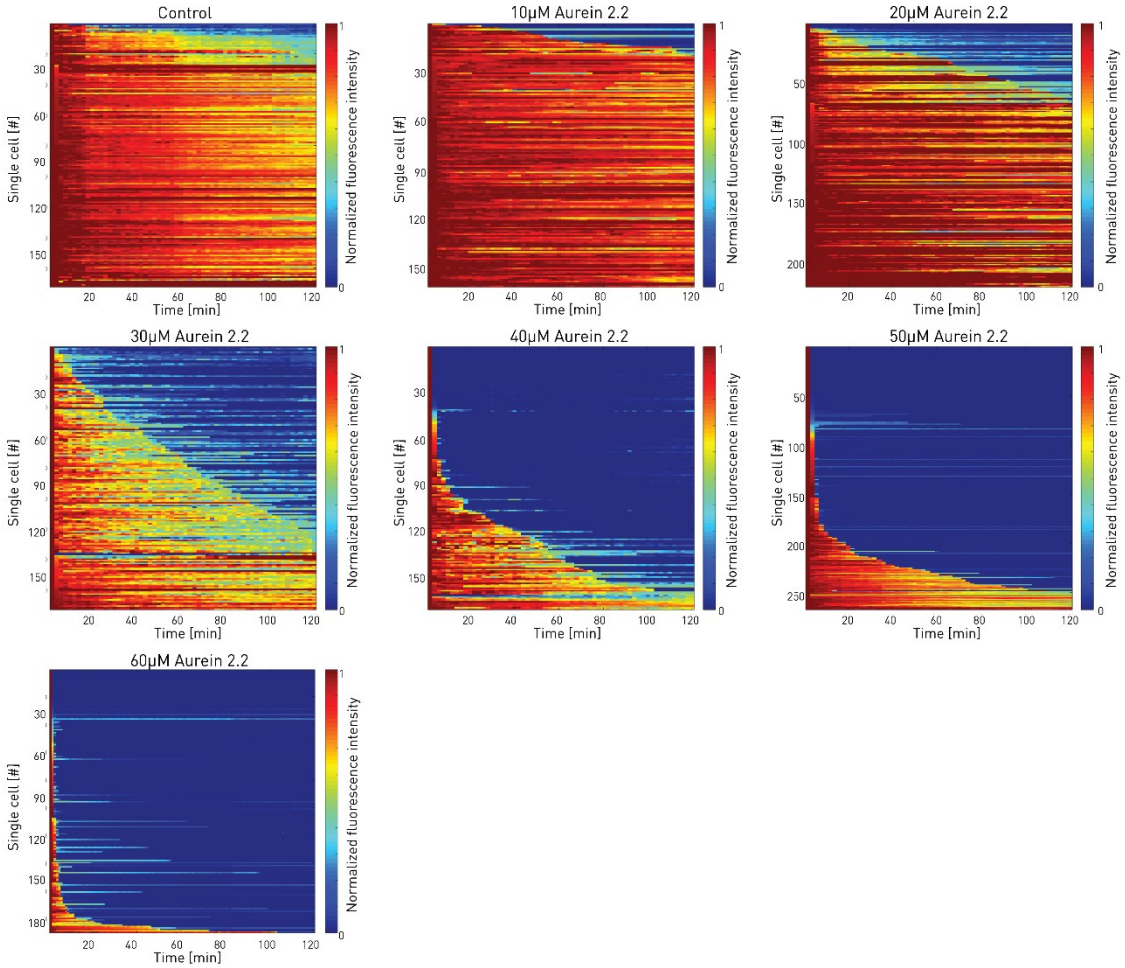

Supplementary Figure S11.

Additional characterization of the cell diameter by evaluation of bright field images taken before the start of the experiments was used to test for correlations between cell size and drug response. Assuming a spherical shape of the cells, correlation with the cell surface area or the cell volume can be investigated as well. For the membranolytic anticancer peptides used in this study, no significant correlation was found for any of the peptides.

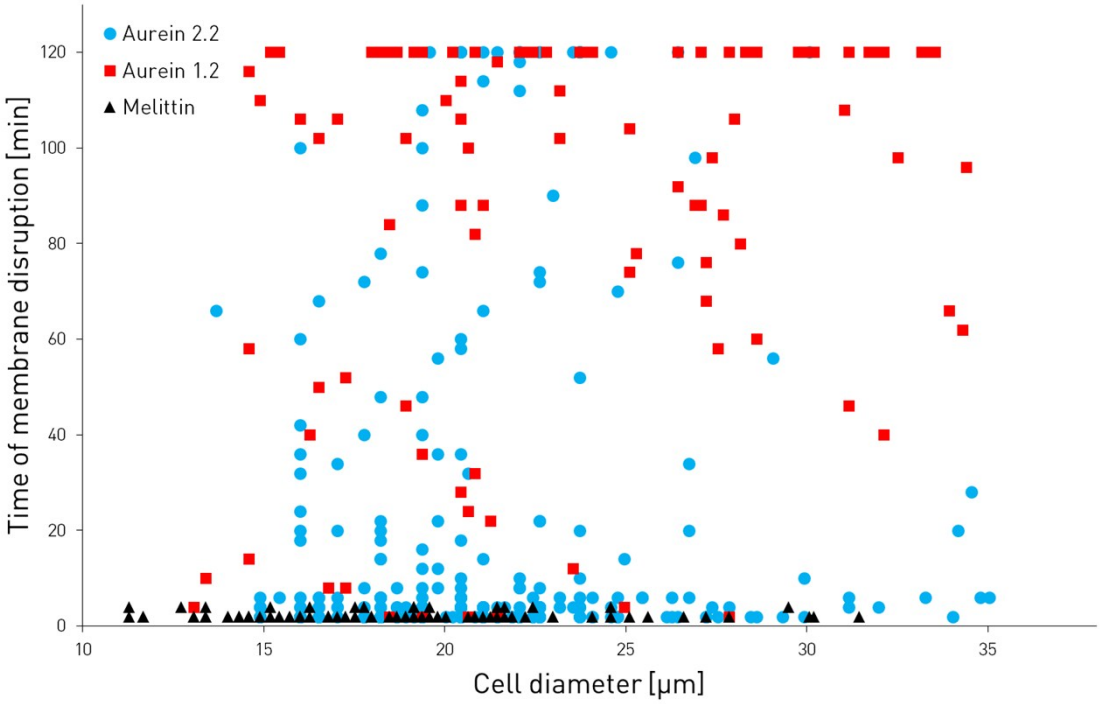

Supplementary Video SV1.

Supplementary video (*.avi format) showing membranolysis of the microfluidic chip. The actuation of the eight individual valves leads to an opening of the corresponding set of valves. Imaging was done at 10 Hz with a 1x objective on a Nikon AZ100M stereo microscope and image acquisition performed with a Nikon Digitalsight Fi1 color camera.

Supplementary Video SV2.

Supplementary video (*.avi format) showing membranolysis of single MCF-7 cells after exposure to the anticancer peptides Melittin (left) and Aurein 2.2 (right), both at 50 µM. Imaging was done at 10 Hz with a 100x oil immersion objective and an Andor iXON Ultra EMCCD camera with a gain of 100 and 50 ms exposure.

Supplementary Video SV3.

Supplementary video (*.avi format) showing the stitched full microfluidic chamber during membranolysis of MCF-7 cells after exposure to 50 µM Aurein 2.2. The fluorescent particles are single cells and the loss of fluorescent signal corresponds to cell death. The video was scaled down by a factor of eight to achieve a reasonable file size.

Supplementary CAD-files SF1.

Electronic CAD file (AutoCAD 2013, *.dwg format) for creating the lithographic mask for microfabrication of the silicon master by photolithography (ESI Figure S1, step 3).